

 Open access • Journal Article • DOI:10.1115/1.1991872

The dynamic response of tuned impact absorbers for rotating flexible structures

— [Source link](#) 

Steven W. Shaw, Christophe Pierre

Institutions: Michigan State University, McGill University

Published on: 01 Jan 2006 - Journal of Computational and Nonlinear Dynamics (American Society of Mechanical Engineers)

Topics: Coefficient of restitution

Related papers:

- [On a Self-Tuning Impact Vibration Damper for Rotating Turbomachinery](#)
- [Performance and dynamic stability of general-path centrifugal pendulum vibration absorbers](#)
- [A centrifugal pendulum absorber for rotating, hollow engine blades](#)
- [Order-Tuned Vibration Absorbers for Cyclic Rotating Flexible Structures](#)
- [Vibration Characteristics of Bladed Disc Assemblies](#)

Share this paper:    

View more about this paper here: <https://typeset.io/papers/the-dynamic-response-of-tuned-impact-absorbers-for-rotating-3uafvrsz51>



The dynamic response of tuned impact absorbers for rotating flexible structures

Steven Shaw, Christophe Pierre

► To cite this version:

Steven Shaw, Christophe Pierre. The dynamic response of tuned impact absorbers for rotating flexible structures. *Journal of Computational and Nonlinear Dynamics*, American Society of Mechanical Engineers (ASME), 2006, 10.1115/1.1991872 . hal-01653840

HAL Id: hal-01653840

<https://hal.archives-ouvertes.fr/hal-01653840>

Submitted on 2 Dec 2017

HAL is a multi-disciplinary open access archive for the deposit and dissemination of scientific research documents, whether they are published or not. The documents may come from teaching and research institutions in France or abroad, or from public or private research centers.

L'archive ouverte pluridisciplinaire **HAL**, est destinée au dépôt et à la diffusion de documents scientifiques de niveau recherche, publiés ou non, émanant des établissements d'enseignement et de recherche français ou étrangers, des laboratoires publics ou privés.



Distributed under a Creative Commons Attribution - NonCommercial| 4.0 International License

THE DYNAMIC RESPONSE OF TUNED IMPACT ABSORBERS FOR ROTATING FLEXIBLE STRUCTURES

Steven W. Shaw*

Department of Mechanical Engineering
Michigan State University
East Lansing, MI 48824–1226
Email: shawsw@egr.msu.edu

Christophe Pierre

Department of Mechanical Engineering
University of Michigan
Ann Arbor, MI 48109-2125
Email: pierre@umich.edu

ABSTRACT

This paper describes an analytical investigation of the dynamic response and performance of impact vibration absorbers fitted to flexible structures that are attached to a rotating hub. This work was motivated by experimental studies at NASA, which demonstrated the effectiveness of these types of absorbers for reducing resonant transverse vibrations in periodically-excited rotating plates. Here we show how an idealized model can be used to describe the essential dynamics of these systems, and used to predict absorber performance. The absorbers use centrifugally induced restoring forces so that their non-impacting dynamics are tuned to a given order of rotation, whereas their large amplitude dynamics involve impacts with the primary flexible system. The linearized, non-impacting dynamics are first explored in detail, and it is shown that the response of the system has some rather unique features as the hub rotor speed is varied. A class of symmetric impacting motions is also analyzed and used to predict the effectiveness of the absorber when operating in its impacting mode. It is observed that two different types of grazing bifurcations take place as the rotor speed is varied through resonance, and their influence on absorber performance is described. The analytical results for the symmetric impacting motions are also used to generate curves that show how important absorber design parameters—including mass, coefficient of restitution, and tuning—affect the system response. These results provide a method for quickly evaluating and comparing proposed absorber designs.

1 Introduction

This paper describes an analysis of a model for a rotating flexible structure fitted with a tuned impact absorber. The absorber is tuned so that at small amplitudes it effectively absorbs vibrations at a given order of rotation, while at larger amplitudes it transitions to an impact damper, wherein it impacts with the structure and utilizes the attendant energy losses to reduce vibration levels. Absorbers of this type have recently been proposed as a means of attenuating vibrations in turbine blades. Their linear response has been analyzed in [1,2] and the impacting response has been investigated in a series of experiments at NASA [3], where the effectiveness of such absorbers has been clearly demonstrated. In this work we carry out a systematic analysis of the response of an idealized system that captures the essential dynamics of the rotating structure and the impact damper, and we focus on the development of methods for predicting the effectiveness of the impact damper for reducing vibration levels. The analytical and simulation results obtained herein can serve as a guide for the selection of absorber parameters in these systems.

Order-tuned absorbers are widely used in rotating machinery, primarily to attenuate torsional vibrations that arise from fluctuating torsional loads. For example, they have a rich history in piston aircraft engines [4], and have more recently been proposed as a method for handling vibrations in advanced-technology automotive engines [5]. In these applications, the absorbers typically consist of masses suspended from the rotor using a bifilar suspension, such that their center of mass travels along a given path (usually circular) relative to the rotor. The selection of the absorber path and its placement on the primary system determine its tuning, both linear and nonlinear. In practice circular paths are used, and the absorbers are linearly tuned to an order slightly higher than that of the dominant order of excitation in order to avoid undesirable nonlinear behavior caused by

*Address all correspondence to this author.

the softening nature of the system, which can result in jump instabilities that turn the absorbers into vibration amplifiers [6, 7]. More recently, it has been proposed to use nonlinear path tuning to avoid these behaviors, and it has been shown that a certain epicycloidal path has some desirable features [8], although it still exhibits certain undesirable instabilities when systems of multiple absorbers are employed [9, 10]. Cycloids have also been proposed, for example, in helicopter applications, with considerable success [11]. A thorough investigation of a wide range of paths shows that slightly overtuned cycloids offer good performance, including avoidance of instabilities and localization of absorber responses, over a wide range of torques [7, 12]. In contrast, in this work these absorbers are used to reduce vibrations in flexible structures that are attached to a rotor that spins at a constant rate.

The basic model for the flexible rotating structure employed here is composed of a pendulum that is attached to a rotating hub via a torsional spring. Thus, the restoring force on the pendulum consists of the elastic component from the spring, as well as centrifugal effects from rotation. In this manner the system has a basic feature required for the present analysis, specifically, a natural frequency that increases as a function of the rotation rate, i.e., it experiences centrifugal stiffening. A pendulum absorber is attached to this primary structure, and is tuned (as described below) to a given order of rotation, as shown in Fig. 1a. Its amplitude is assumed to be limited by stops which are fixed to the primary pendulum, representing the absorber’s rattle space constraints. Upon contact with the stops, momentum is transferred between the absorber and the primary system, and energy is dissipated. This simplified model allows one to analytically predict both the linear (non-impacting) response and the desired type of non-linear response, that is, one in which the absorber mass bounces back and forth between its limits in a symmetric manner. Parameter studies are conveniently carried out by analyzing the steady-state responses of this idealized model, and the results are compared with simulations of the system.

The paper is organized as follows. In Section 2 the model is described, the equations of motion are presented in dimensionless form, and the nondimensional system parameters are defined. Section 3 contains an analysis of the linearized (non-impacting) response, explores some interesting features of the linear system response, and shows how the absorber is tuned to function at small amplitudes. A nonlinear analysis of the desired symmetric impacting motions is given in Section 4. Section 5 shows sample results for various parameter conditions in the form of plots of structural response amplitude versus rotation speed. These results, which are verified by numerical simulations, demonstrate the effectiveness of the absorber in attenuating the structural resonance that occurs as the speed passes through the resonance of the flexible structure. The paper closes with some remarks and directions for future work in Section 6.

2 Equations of Motion

An idealized model is developed here, but, as shown in Section 5, it possesses the important features required to mimic actual implementations of these absorbers. The model to be considered is shown in Fig. 1a. The primary system consists of a rigid massless bar of length L and end-mass M that is attached via a linear torsional spring of stiffness K_t to a hub at a distance R from the hub center. The hub is assumed to be rotating about a fixed axis at a constant rate Ω . It is also assumed that when the pendulum has a purely radial configuration, that is, $\theta = 0$, the torsional spring is unstressed. This primary system pendulum is periodically excited by a transverse force applied at the end-mass, with a frequency that is linked to the rotation rate, i.e., $F(t) = F_0 \sin(n\Omega t)$ where n is the so-called engine excitation order, typically an integer or a simple fraction [13]. Reducing the vibratory response of this primary system, especially at resonance conditions, is the main objective of this work.

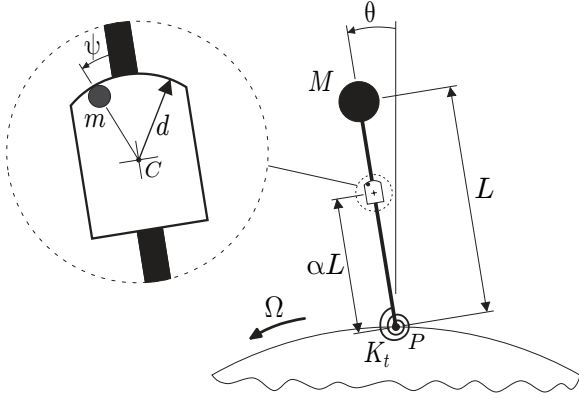
The absorber can be conveniently modeled by another pendulum, taken to be of length d and mass m (typically $m \ll M$) that is attached to the primary pendulum bar at a distance αL from its pivot, where $0 < \alpha < 1$. The absorber pendulum angle ψ has its amplitude limited to a value of ψ_0 by stops, which represents the rattle space limits found in typical turbine blades. Note that this pendulum is dynamically equivalent to the hardware implemented in practice, which consists of a mass moving along a machined surface [3] that impacts the blade at a certain amplitude.¹ The absorber length d will be selected to provide small amplitude tuning at the desired order, exactly as for the centrifugal pendulum absorbers used to attenuate torsional oscillations in rotating systems [7]. When the absorber makes contact with a stop, momentum is exchanged between the absorber and the primary system, and energy dissipation is modeled using a coefficient of restitution.

Damping ratios for the structures of interest are very low, typically in the range 0.1% or less of critical damping. In addition, it is desired to keep the absorber damping as small as possible, since it remains tuned to the desired order at all rotation speeds. Thus, energy dissipation in this system is dominated by impacts.

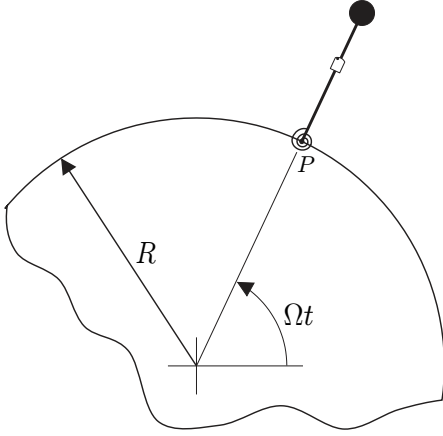
2.1 Motion Between Impacts

The equations of motion for this system between impacts are derived using a Lagrangian approach and linearized for small angles of both the primary and absorber pendulums, that is, for small θ and ψ . They are divided through by their respective inertia terms and time is rescaled using the mechanical natural frequency of the isolated primary system at zero rotor speed, ω_0

¹It should be noted that in [3] spherical balls are used for the absorber mass, and these presumably roll without slipping, in which case their effective mass will include rotational effects; see [8] for a similar analysis involving the rollers of bifilar torsional absorbers.



(a) Blade Model with Absorber



(b) System Attached to Rotating Hub

Figure 1. (a) Schematic diagram of the pendulum-type blade model with attached pendulum absorber. (b) System attached to the rotating hub.

(defined below). This yields a pair of dimensionless linear equations that describe the motion between impacts, as follows,

$$\mathbf{M}\ddot{\mathbf{z}} + \mathbf{C}\dot{\mathbf{z}} + \mathbf{K}\mathbf{z} = \mathbf{f} \quad (1)$$

where an overdot indicates a derivative with respect to dimensionless time τ (defined below), and the dynamic variables are defined to be $\mathbf{z} = (x, y)^T = (\theta/\psi_0, \psi/\psi_0)^T$, and have been chosen such that impacts occur at $|y| = 1$. The dimensionless symmetric

mass and stiffness matrices have elements given by

$$\begin{aligned} M_{11} &= 1 + \mu(\alpha + \gamma)^2, \\ M_{12} &= M_{21} = \mu\gamma(\alpha + \gamma), \\ M_{22} &= \mu\gamma^2, \\ K_{11} &= 1 + \delta\sigma^2(1 + \mu(\alpha + \gamma)), \\ K_{12} &= K_{21} = \delta\mu\gamma\sigma^2, \\ K_{22} &= \mu\gamma\sigma^2(\alpha + \delta), \end{aligned}$$

and the force vector is given by

$$\mathbf{f} = (f \cos(n\sigma\tau), 0). \quad (2)$$

A number of dimensionless system parameters have been introduced, which are now described. There are three length ratios: the pendulum length $\gamma = d/L$, the hub radius $\delta = R/L$, and the absorber pendulum pivot location along the primary system α (recall that α was initially defined as a length ratio in terms of L). The ratio of absorber to primary system mass is described by $\mu = m/M$. The normalized amplitude of the applied moment due to the force acting on the primary mass is given by $f = FL/(K_t\psi_0)$, and the rescaled time is given by $\tau = \omega_0 t$ where $\omega_0 = \sqrt{K_t/M}/L$ is the natural frequency of the isolated primary system at zero rotational speed, that is, $\Omega = 0$. The rotational speed has also been nondimensionalized using this frequency and is described by the parameter $\sigma = \Omega/\omega_0$. Of primary interest is the response of the primary system as σ varies, especially near resonance conditions.

The parameter γ is a measure of the effective absorber pendulum length (or, equivalently, the curvature of the absorber path), while $(\alpha + \delta)$ is a measure of the distance from the center of rotation to the absorber attachment point. These two geometric quantities will be central to the order tuning of the absorber. In practice the absorber mass is small compared to that of the primary system, such that μ is typically of the order $10^{-2} - 10^{-3}$. Similarly, due to the scaling used, the dimensionless force amplitude f will also be small. In terms of the frequency scaling, note that resonance will nominally occur when one of the excitation orders $n\sigma$ matches a natural frequency of the system. In the absence of centrifugal stiffening of the primary system, this occurs for the primary system without the absorber whenever $n\Omega = \omega_0$, which corresponds to $\sigma = 1/n$. This resonance condition is shifted slightly by centrifugal stiffening effects, as described below. Finally, note that in the absence of rotation ($\sigma = 0$), the stiffness matrix has only one nonzero element, related to K_t .

The system damping can be modeled in a number of ways, but in general the details are not crucial since the damping ratios of the primary system and the absorber are both very small. In fact, damping is ignored in most of the present analysis, where

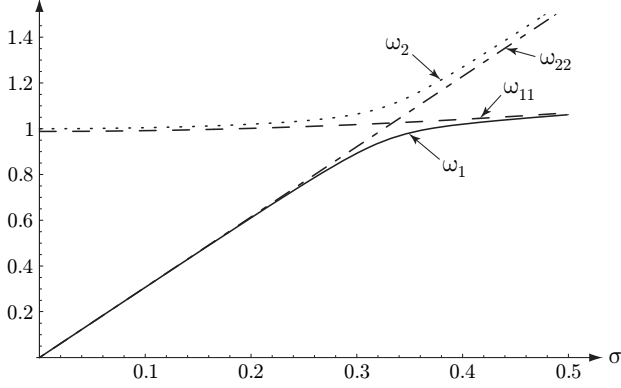


Figure 2. Normalized linear natural frequencies versus normalized rotation rate σ . The dashed line is the primary system frequency with the absorber locked, ω_{11} , showing centrifugal stiffening; the dashed-dotted line is the absorber frequency with the primary system locked, $\omega_{22} = \tilde{n}\sigma$; the solid and dotted lines represent the in-phase and out-of-phase system natural frequencies, ω_1 and ω_2 , respectively. Note the veering that occurs for small absorber mass. Parameter values: $\mu = 0.024$, $\delta = 0.67$, $\alpha = 0.84$, $\tilde{n} = 3.007$.

the dominant source of energy dissipation are losses incurred by the impacts of the absorber with the primary system. However, when primary system and absorber damping are to be included in the analysis or simulations, we do so by adopting simple modal damping, rather than using a particular form for the damping matrix \mathbf{C} .

Figure 2 shows the following four frequencies as functions of the rotation rate σ : the two natural frequencies, ω_1 and ω_2 (obtained in the usual manner from the mass and stiffness matrices given above); the natural frequency of the primary system with the absorber locked, ω_{11} (derived below); and the natural frequency of the absorber with the primary system locked, ω_{22} (also derived below). It is interesting to note that for small values of the mass ratio, the two natural frequencies lie close to ω_{11} and ω_{22} , and exhibit a classical eigenvalue veering behavior [14]. The close proximity of a natural frequency to the absorber tuning frequency ω_{22} can be of concern when designing absorbers, an issue considered subsequently.

Figure 3 shows the modal amplitude ratios versus σ , expressed in terms of the ratio $r_i = (x/y)_i (= \theta/\psi)_i$ for the $i = 1, 2$ modes. Note that the in-phase mode starts at $\sigma = 0$ as a rigid body mode, near the “primary system locked” mode, while the out-of-phase mode starts near the “absorber locked” mode (due to $\mu \ll 1$). As σ increases, the eigenvalue veering takes place near the resonant rotor speed $\sigma \cong 1/n$, and as $\sigma \rightarrow \infty$ the roles of the modes switches such that the in-phase mode is asymptotic to the “absorber locked” mode while the out-of-phase mode is asymptotic to the “primary system locked” mode. It is interesting to note that the first natural frequency of the full system ω_1

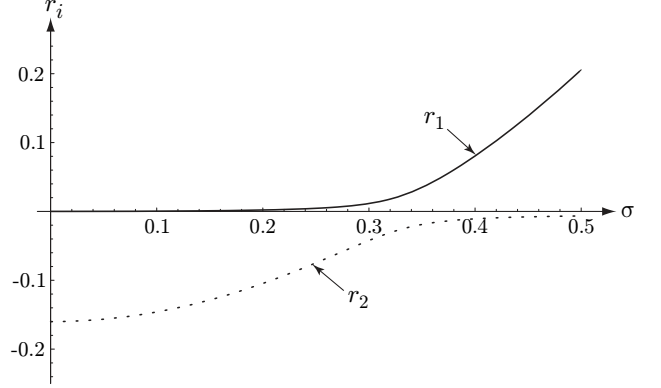


Figure 3. Modal amplitude ratios as a function of σ ; line types and parameters are the same as those in Fig. 2.

follows ω_{22} for small σ values and then switches branches and approaches ω_{11} as $\sigma \rightarrow \infty$. Similarly, ω_2 follows ω_{11} for small σ values and then switches branches and tracks closely ω_{11} as σ becomes large. However, numerical plots show that in this latter case the two branches have a very slight difference in their large- σ asymptotic slopes. This effect has some interesting consequences that are more fully explored in [15].

The steady-state response of these linear equations of motion is considered in detail in Section 3.3.

2.2 Impact Dynamics

The linear differential equations of motion are valid for $|y| < 1$ and impacts occur at $|y| = 1$. Using conservation of angular momentum about the rotation center and a simple Newtonian impact law involving the relative normal velocities of the primary system and the absorber, it can be shown that, for small angles, the angular velocities before (superscript $-$) and after (superscript $+$) impact are related as follows,

$$\left. \begin{aligned} \dot{x}^+ &= \dot{x}^- + E\dot{y}^- \\ \dot{y}^+ &= -e\dot{y}^- \end{aligned} \right\}, \quad (3)$$

where e is the usual coefficient of restitution, $0 \leq e \leq 1$, and

$$E = \frac{\gamma\mu(1+e)(\alpha+\delta+\gamma)}{1+\delta+\mu(\alpha+\gamma)(\alpha+\gamma+\delta)}. \quad (4)$$

Note that the impact rule for the absorber mass is very simple due to the fact that it is measured relative to the angular displacement of the primary system. Also note that the velocity of the primary system undergoes a jump at impact, and that the magnitude of the jump is proportional to the mass ratio μ , as expected from such a momentum transfer. Similar models for translational impact

absorbers have been the subject of previous investigations; see, for example, [16, 17].

The equations of motion between impacts and these impact relations form the basis of the analysis to follow. We begin by analyzing the linear response of the system, which is valid for steady-state amplitudes below the impact threshold. This analysis sets the stage for the dynamics with impacts, which are considered in Section 4.

3 Response of the Linear System

Some special cases of interest are considered first, after which we turn to the general situation. The first special case is the system wherein the absorber is locked in place at its zero position relative to the primary system. The steady-state response from this case is used to provide a baseline for assessing the effectiveness of the absorber.² We then consider the primary system locked at its zero position, with the absorber free to move. From this free vibration situation one can determine the natural frequency of the isolated absorber, which is directly related to the linear tuning the absorber. Finally, we consider the response of the general system in which the primary system and the absorber are both free to move. From this we determine the motions that do not involve impacts, describe the rather interesting resonance structure of the system, and determine conditions under which impacts must occur.

3.1 The Absorber Locked

Consider the response of the primary system, that is, the x -dynamics, with the absorber locked at its zero position, $y = 0$. The response of this periodically forced single degree of freedom system will be used for comparisons when evaluating the effectiveness of the absorber. This system also allows one to consider the isolated primary system, simply by taking $\mu = 0$.

The equation of motion for the primary system with the absorber mass fixed to it is found by setting $y \equiv 0$ in the equations of motion and including a constraint force acting on the absorber to hold it in place. (See the appendix for a more complete discussion of this force, which is utilized in the simulations.) The resulting equation for the motion of the primary system is given by

$$M_{11}\ddot{x} + K_{11}x = f \cos(n\sigma\tau), \quad (5)$$

which is a harmonically forced simple harmonic oscillator with a natural frequency $\omega_{11} = \sqrt{K_{11}/M_{11}}$ that depends on the rotation rate through σ . An example of this frequency versus the spin rate

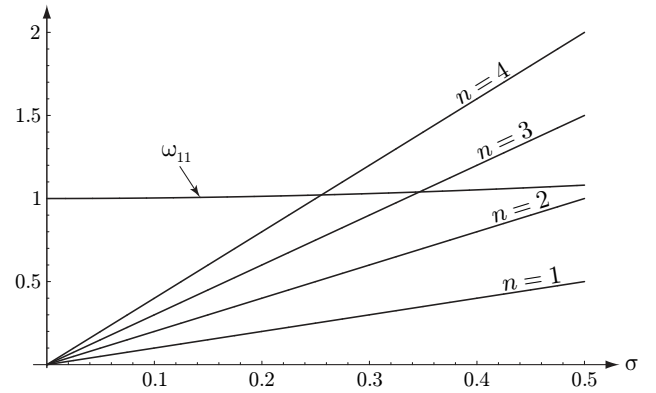


Figure 4. Campbell diagram. Primary system frequency (with no absorber) versus σ along with order excitation lines for $\mu = 0$, $\delta = 0.67$, and orders $n = 1, 2, 3$, and 4.

σ is shown in Fig. 2. Note that when $\mu = 0$, that is, when the absorber is removed, this frequency is given simply by $\sqrt{1 + \delta\sigma^2}$, which demonstrates in a simple form the centrifugal stiffening effects of the primary system (for small μ this is, in fact, a very good approximation for ω_{11}). The term $\delta\sigma^2 = (RML/K_I)\Omega^2$ captures these effects.

A resonance for the primary system occurs whenever $n\sigma = \omega_{11}$, which can be solved to determine the rotational speeds at which resonances occur. A typical diagram showing resonance conditions for a few values of the excitation order n is shown in Fig. 4 (for $\mu = 0$). Note that only the $n = 3$ and 4 orders (of those shown) excite the primary system over the spin range depicted. Without the absorber present ($\mu = 0$), this resonance condition is given simply by $\sigma = \sqrt{1/(n^2 - \delta)}$, which is slightly shifted upwards from $\sigma = 1/n$, due to centrifugal stiffening effects. Note that since the primary system is modeled by a single mode, there exists a single resonance speed for each excitation order, as can be verified by considering the intersections points in Fig. 4. The resonance situation for the system with the absorber free to move is significantly more subtle, as described subsequently.

The response of this baseline system as one varies the rotational speed σ is that of a linear oscillator (whose natural frequency depends on the spin rate), forced by harmonic excitation at a frequency proportional to the spin rate. (Examples of these response curves are given later, when used for comparison purposes.) At resonance the response will be limited in amplitude by the (typically very small) damping in the primary system, and/or by nonlinear effects. The impact absorbers are designed to handle precisely these resonances. In the numerical examples that follow, we focus on the $n = 3$ resonance.

3.2 The Primary System Locked

Here we take $x = 0$ and consider the y -dynamics. These are free vibrations of the absorber acting under the influence of

²This system is used for reference since it includes the inertia of the absorber as fixed to the primary system, but not its dynamics relative to the primary system.

the constant rotation rate of the hub, which are governed by the equation of motion

$$M_{22}\ddot{y} + K_{22}y = 0. \quad (6)$$

This system has a dimensionless natural frequency of

$$\omega_{22} = \sigma \sqrt{\frac{\alpha + \delta}{\gamma}} = \sigma \tilde{n}, \quad (7)$$

where

$$\tilde{n} = \sqrt{\frac{\alpha + \delta}{\gamma}} \quad (8)$$

is the tuning order of the absorber, determined by selecting the length of the pendulum absorber γ (dimensionally d), and the distance of its attachment point from the center of rotation ($\alpha + \delta$) (dimensionally $\alpha L + R$). It is important to note that the sole restoring force for the absorber arises from centrifugal effects, and this results in a natural frequency that is directly proportional to the rotation rate σ . This frequency is shown in Fig. 2 for a case where it is tuned to $\tilde{n} = 3.007$, which will be used to address excitation forces of order $n = 3$ in the subsequent parameter study. This restoring force allows the absorber to be tuned to a given order, rather than to a given frequency. Just as in the case of translational absorbers, one selects the isolated absorber frequency to meet a certain tuning condition. In the present case, in order to address an excitation of order n , absorber parameters are selected such that $\tilde{n} \approx n$. In fact, linear theory would dictate $\tilde{n} = n$, but it is known that such absorbers should be slightly detuned in order to avoid finite amplitude and localization effects [6, 7, 12]. In addition, it is known that if one can maintain the absorber frequency close to the excitation frequency, an absorber is most effective when lightly damped. For these order-tuned absorbers this is precisely the situation.

In the following analysis, the pendulum length parameter γ is replaced by the tuning parameter \tilde{n} , using the substitution

$$\gamma = (\alpha + \delta) / \tilde{n}^2. \quad (9)$$

This allows one to see more directly the effects of absorber tuning in the analytical results.

3.3 The General System

For $|y| < 1$ the two degree of freedom system with the primary system and the absorber free to move has a steady-state response of the form

$$\begin{bmatrix} x_{ss} \\ y_{ss} \end{bmatrix} = \begin{bmatrix} X \\ Y \end{bmatrix} \cos(n\sigma t), \quad (10)$$

where

$$\left. \begin{aligned} X &= \frac{-f(\alpha + \delta - \gamma n^2)}{\Gamma} \\ Y &= \frac{f(\delta - (\alpha + \gamma)n^2)}{\Gamma} \end{aligned} \right\} \quad (11)$$

with

$$\begin{aligned} \Gamma &= \alpha^3 \mu n^2 \sigma^2 + \alpha^2 \mu (2\gamma n^2 + \delta(-1 + n^2)) \sigma^2 \\ &\quad - (\delta - \gamma n^2) (1 + \delta \sigma^2 - n^2 \sigma^2) \\ &\quad + \alpha \left(-1 - \delta^2 \mu \sigma^2 + (1 + \gamma^2 \mu) n^2 \sigma^2 \right. \\ &\quad \left. + \delta(-1 + \gamma \mu(-1 + n^2)) \sigma^2 \right). \end{aligned}$$

Note that the phases are automatically accounted for in this undamped system by the signs of (X, Y) . This result can also be expressed in terms of the absorber tuning by replacing γ using Eq. (9). This yields

$$\left. \begin{aligned} X &= \frac{f \tilde{n}^2 (\tilde{n}^2 - n^2) (\alpha + \delta)}{\tilde{\Gamma}} \\ Y &= \frac{f \tilde{n}^2 (\delta (n^2 - \tilde{n}^2) + \alpha n^2 (1 + \tilde{n}^2))}{\tilde{\Gamma}} \end{aligned} \right\}, \quad (12)$$

where $\tilde{\Gamma}$ is simply Γ with γ replaced using Eq. (9).

It is interesting to note that this system experiences at most a single resonance as the rotor spins up, that is, as σ varies. This is due to the fact that the natural frequencies depend on σ , and if one considers a straight line representing an order excitation superimposed in Fig. 2, it is seen that it will cross at most one of the system natural frequency curves. Especially interesting is the situation when the absorber is tuned to be close to the order of the excitation, as is typically the case in practice. In this case the order excitation line $n\sigma$ lies very close to the absorber frequency line $\tilde{n}\sigma$, and thus the resonance condition is very sensitive to small changes in the absorber tuning. (In Fig. 2 this is

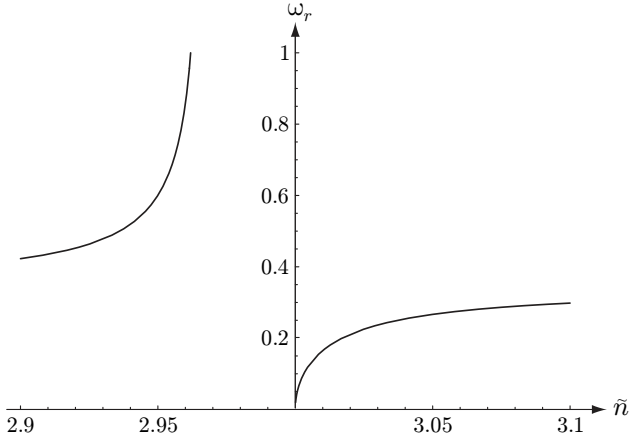


Figure 5. System resonance frequency versus \tilde{n} . Parameter values: $\mu = 0.024$, $\delta = 0.67$, $\alpha = 0.84$, $n = 3$.

precisely the situation, where the absorber is tuned to $\tilde{n} = 3.007$ in order to address order $n = 3$ excitation). As one varies the absorber tuning \tilde{n} around n , the intersection point between the order excitation line $n\sigma$ and the natural frequency curves ω_1 and ω_2 moves in a complicated manner, and even has a range of values for which no intersection exists, leading to a discontinuity in the resonance condition. This dependence can be determined by solving for the σ values at which $\tilde{\Gamma} = 0$, corresponding to the system natural frequencies. The result is shown graphically in Fig. 5, which depicts the resonance frequency ω_r as a function of \tilde{n} for $n = 3$. By examination of this plot, along with Fig. 2 and Fig. 3, it is seen that when $\tilde{n} > n$ the in-phase mode is excited at resonance, while for $\tilde{n} < n$ the out-of-phase mode is excited at resonance below a certain threshold, but that between this threshold and perfect tuning no resonance will occur. (For the parameters given this threshold occurs at $\tilde{n} \cong 2.9665$.) Therefore, one must take note that distortions due to stress, thermal effects and/or wear may have a significant effect on the system response when the absorber is tuned to be very close to the excitation order. If the absorber is designed to operate in a non-impacting manner, one can make the absorber design robust to nonlinear effects and small uncertainties by selecting the absorber tuning to be slightly *higher* than the ideal value [6, 7, 12]. This is in direct contrast to order-tuned absorbers used for reducing torsional vibrations, which should be slightly undertuned [7].

The desired tuning of the absorber is achieved by selecting absorber parameters such that X is as small as possible over a range of excitation parameters. For this undamped model, the state $X = 0$ can be achieved over all rotation rates by selecting the system geometric parameters to satisfy $\tilde{n} = n$. If one takes the pendulum length γ to be the physical parameter of choice, the

perfect tuning condition is given by,

$$\gamma = \bar{\gamma} = \frac{\alpha + \delta}{n^2} \quad \text{or, equivalently,} \quad \tilde{n} = n. \quad (13)$$

This fixes the absorber pendulum length d to be a specific proportion of the distance of its pivot point from the center of rotation, $(\alpha L + R)$. The constant of proportionality is given by $1/n^2$, that is, it is dictated by the desired tuning order n in such a manner that higher order absorbers will have smaller effective lengths. This tuning is the same as the case when these absorbers are used to attenuate rotor torsional vibrations of order n [7, 18].

It is important to note that this tuning is valid at all rotation speeds, which is made possible since the frequency of the absorber is proportional to the rotation speed σ . When tuned in this manner, the absorber moves at the frequency of the applied force, and exactly out of phase with respect to it. The absorber amplitude at this condition, and with $\tilde{n} = n$, is given by

$$\bar{Y} = Y(\tilde{n} = n) = \frac{-fn^2}{\alpha\mu\sigma^2(\alpha + \delta)(1 + n^2)}. \quad (14)$$

This absorber amplitude results in an absorber moment acting on the primary system that precisely cancels the applied moment. Note that if small damping is considered in the absorber, the condition $X = 0$ cannot be met, and there will be a small residual vibration in the primary system, accompanied by a phase shift. Also, the condition $X = 0$ cannot be met when small intentional mistuning is employed, although the residual vibrations are the tradeoff for significantly more robust operation.

Note also that the amplitude of the absorber is inversely proportional to the mass ratio μ , which is generally small. This leads to a limited range of force amplitudes over which the system dynamics remain linear. Beyond the linear range, one must consider nonlinearities in the absorber motion. These can include effects from the absorber path, as is done for torsional absorbers [7], or, as in the current work, the effects of impacts with motion-limiting barriers [19].

As the force amplitude is increased, the absorber will eventually run out of rattle space, at which point the impact functionality of the absorber takes over. A force level above which the absorber mass will necessarily impact in steady-state can be derived from the linear results by taking $|Y| = 1$ in Eq. (12) and solving for $f = f_{cr}$. The results of f_{cr} versus σ for three values of absorber tuning are depicted in Fig. 6. It is noted that there is a zero force threshold at a particular value of σ in the case $\tilde{n} = 3.007$; this corresponds to a system resonance, at which point the undamped system amplitude is unbounded for any (nonzero) level of force. For the perfectly tuned case, $\tilde{n} = 3$, the zero force threshold occurs only for zero rotor speed. In contrast, for

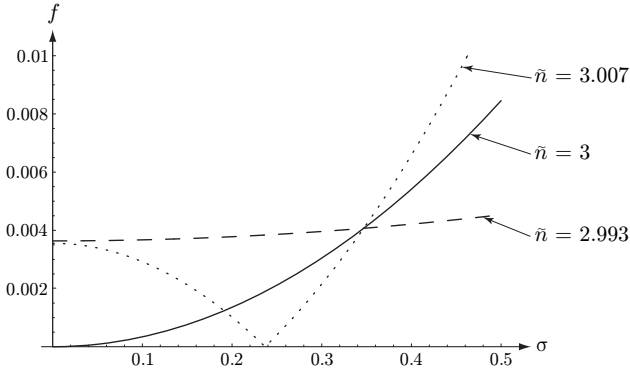


Figure 6. Excitation force amplitude thresholds above which impacts must occur, depicted as f versus σ , for absorber tuning values $\tilde{n} = 2.993$ (dashed line), $\tilde{n} = 3$ (solid line), and $\tilde{n} = 3.007$ (dotted line). The non-impacting steady-state response exists below these curves, and impacting motions must occur above them. Note that impacting and non-impacting steady-state responses can co-exist below these curves. Parameter values: $\mu = 0.024$, $\delta = 0.67$, $\alpha = 0.84$, $n = 3$.

$\tilde{n} = 2.993$, a case for which no resonance occurs, there is a finite critical force amplitude for all rotor speeds.

In general, one must note that above this threshold impacts must occur in steady-state operation, but that steady-state impacting motions can also exist below this critical force level. In these situations the non-impacting steady-state response co-exists with one or more impacting steady-state responses, leading to hysteresis in the response as parameters are varied across this threshold. The overall picture of the nonlinear system response is considered more fully next.

4 Periodic Impact Response

We now turn to the response of the system when the absorber undergoes impacts. Systems with impacts have been widely studied, and much is known about their dynamics, which can be quite rich in terms of complicated bifurcation patterns, the existence of chaos, multiple coexisting steady-state responses, and bifurcations that are unique to such systems, such as grazing bifurcations [16, 20–23]. The equations of motion that govern the impacts are derived above, and can be used for simulation studies. In this section we focus on the steady-state impacting motions in which the absorber moves in a symmetric manner between its limits with a period equal to that of the excitation. An example of such a motion, shown as trajectories in the individual (y, \dot{y}) and (x, \dot{x}) phase planes, is presented in Fig. 7. This is the simplest of the many possible impacting steady-states, and it lends itself naturally to analytical treatment. In addition, it is the desired motion of the absorber, since it represents the nonlinear continuation of the linear response of the absorber, and, in fact, it is the most widely observed type of steady-state encountered

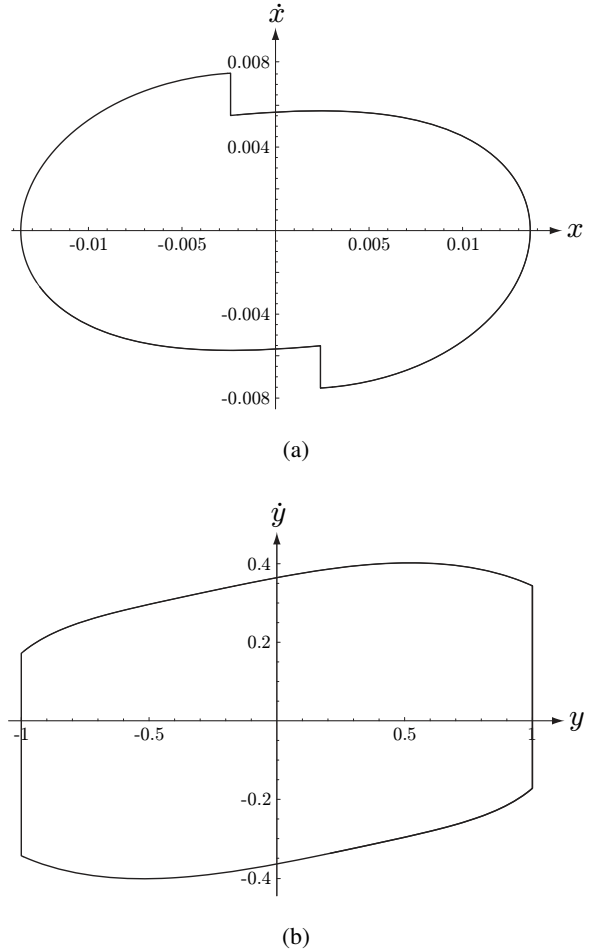


Figure 7. A typical symmetric periodic impacting response. (a) \dot{x} versus x . (b) \dot{y} versus y . Parameter values: $\mu = 0.024$, $\delta = 0.67$, $\alpha = 0.84$, $\tilde{n} = 3.007$, $n = 3$, $e = 0.5$, $f = 0.01$, $\sigma = 0.17$ and modal damping ratios of 1.0%.

in simulations.

Before starting the analysis, it is worthwhile to point out where such motions are expected to occur. Figure 6 provides a useful guide for this issue. First, consider an absorber system that is undertuned, such as $\tilde{n} = 2.993$, corresponding to the dashed line in Fig. 6. If the force amplitude is small, below approximately $f = 0.004$ in this case, the nonimpacting steady-state response is feasible and should dominate the system behavior. For $f \gtrsim 0.004$ the response will be dominated by impacts, since the nonimpacting steady-state response exceeds the rattle-space limits. If one considers the perfectly tuned absorber, $\tilde{n} = 3$, corresponding to the solid line in Fig. 6, it is seen that there exists a critical rotor speed above which the nonimpacting steady-state response exists. Coexisting with this response over at least part of this region are a pair of symmetric impacting responses, one sta-

ble and one unstable. As the rotor speed is decreased from above the threshold curve, the absorber non-impacting response amplitude approaches unity and only impacting motions will occur below the threshold. In fact, at the threshold curve the linear non-impacting response joins with the unstable symmetric impacting response via a grazing type of saddle-node bifurcation, annihilating them both [21].³ For rotor speeds less than the threshold, the stable symmetric impacting continues to exist. This situation, wherein there are two possible stable steady-state responses beyond the threshold, leads to that hysteresis in the response as the rotor speed varies. The most interesting case is that of overtuned absorbers, such as the dotted curve in Fig. 6, corresponding to $\bar{n} = 3.007$. In this case a system resonance occurs at a rotor speed of approximately $\sigma = 0.24$, corresponding to the vertex of the V-shaped wedge in the force threshold curve. In this case the nonimpacting steady state exists in rotor speed zones both below and above the resonance, and impacting is guaranteed to occur only in a range about the resonance. As the rotor speed is increased from zero, the nonimpacting response initially exists, and at the first threshold crossing it transitions to a stable symmetric impacting motion via a grazing contact. As the rotor speed is further increased, the second threshold is encountered, and the behavior about this curve is qualitatively the same as that described for the perfectly tuned case.

The symmetric impacting motions can be investigated using analytical techniques. The approach taken here is to use matching conditions to determine conditions for which this response exists and examine how it affects the vibration of the primary structure. (See, for example, [16, 17, 20] for similar analyses.) In particular, it is of interest to know whether or not the absorber serves to reduce the resonance of the primary system when responding with impacts, and if so, to determine its effectiveness. With such results, one can carry out parameter studies to determine absorber parameters that lead to good performance.

A symmetric periodic response of the absorber will satisfy certain matching conditions, and these can be used to analytically determine the response and its stability. In this section we analytically determine the conditions for the existence of such solutions, and leave the determination of stability to simulations. To this end, the system response displacements during free flight, that is, between impacts, are expressed as

$$\left. \begin{aligned} x(t) &= x(t; t_0, x_0, \dot{x}_0, y_0, \dot{y}_0) \\ y(t) &= y(t; t_0, x_0, \dot{x}_0, y_0, \dot{y}_0) \end{aligned} \right\}, \quad (15)$$

where the initial conditions are taken to be $(x, \dot{x}, y, \dot{y})|_{t=t_0} = (x_0, \dot{x}_0, y_0, \dot{y}_0)$. Now consider a response which starts at time

³Grazing refers to a zero-velocity impact. As will be demonstrated in the simulations below, another type of grazing bifurcation occurs in this system, one that leads directly to chaos.

$t = t_0$ with the absorber at its right limit, $y(t_0) = y_0 = 1$, with negative absorber velocity, $\dot{y}(t_0) = \dot{y}_0 < 0$, along with initial conditions $(x(t_0), \dot{x}(t_0)) = (x_0, \dot{x}_0)$ for the primary system. The absorber will move to the left and strike the left limit at a time t_1 , whereupon $y(t_1) = -1$ with velocity $\dot{y}(t_1) < 0$ and $(x(t_1), \dot{x}(t_1))$ for the position and velocity of the primary system. The system dynamical states immediately after the impact are determined from those immediately before the impact by applying the impact rule given in Eq. (3). In order for this response to be periodic and symmetric between subsequent impacts, the following conditions must hold: the time of flight $t_1 - t_0$ equals one-half the period of the excitation (or N times one-half the period for an order N subharmonic response), and the system states just after an impact at $y = -1$ ($y = 1$, respectively) are the negative of those just after the preceding impact at $y = 1$ ($y = -1$, respectively). These periodicity conditions hold only for special values of the initial conditions, which are indicated here by an overbar. These conditions are derived by using the linear free-flight solutions and the inverse of the impact conditions, and can be expressed as follows,

$$\begin{aligned} x(\bar{t}_0 + T/2; \bar{t}_0, \bar{x}_0, \bar{\dot{x}}_0, \bar{y}_0 = 1, \bar{\dot{y}}_0) &= -\bar{x}_0 \\ \dot{x}(\bar{t}_0 + T/2; \bar{t}_0, \bar{x}_0, \bar{\dot{x}}_0, \bar{y}_0 = 1, \bar{\dot{y}}_0) &= -\bar{\dot{x}}_0 - E\bar{y}_0/e \\ y(\bar{t}_0 + T/2; \bar{t}_0, \bar{x}_0, \bar{\dot{x}}_0, \bar{y}_0 = 1, \bar{\dot{y}}_0) &= -\bar{y}_0 (= -1) \\ \dot{y}(\bar{t}_0 + T/2; \bar{t}_0, \bar{x}_0, \bar{\dot{x}}_0, \bar{y}_0 = 1, \bar{\dot{y}}_0) &= \bar{\dot{y}}_0/e \end{aligned}$$

where $T = 2\pi/(n\sigma)$ is the forcing period. Note that these equations are necessary, but not sufficient, for the existence of a symmetric two-impact periodic solution. In particular, one must ensure that the absorber response stays bounded within its limits between impacts, that is,

$$|y(t; \bar{t}_0, \bar{x}_0, \bar{\dot{x}}_0, \bar{y}_0 = 1, \bar{\dot{y}}_0)| < 1, \quad \forall t \in (\bar{t}_0, \bar{t}_0 + T/2). \quad (16)$$

If this condition is violated, the mathematical solution exceeds the limits during part of the motion, and is thus nonphysical [24].

It is interesting to note the structure of the four matching equations. The functions for $x(t)$, etc., are taken from the solution of the linear free-flight vibration problem. The unknowns in the equations are the initial conditions $(\bar{t}_0, \bar{x}_0, \bar{\dot{x}}_0, \bar{y}_0)$ that result in a periodic response. (Note that the initial condition on y is known, since we start at the limit $y(t_0) = y_0 = 1$.) The unknowns represent the phase of the forcing, the displacement and velocity of the primary system, and the velocity of the absorber, all evaluated immediately after an impact at $y = 1$. The equations can be expanded using trigonometric identities such that they are linear in the following terms: $(\bar{x}_0, \bar{\dot{x}}_0, \bar{y}_0, \sin(n\sigma\bar{t}_0), \cos(n\sigma\bar{t}_0))$. The solution procedure involves eliminating two of the first three terms using two of the equations, and then solving the remaining two equations for $\sin(n\sigma\bar{t}_0)$ and $\cos(n\sigma\bar{t}_0)$. Then, using

$\cos^2(n\sigma\bar{t}_0) + \sin^2(n\sigma\bar{t}_0) = 1$, one is left with a single quadratic function of the remaining variable, which can be solved. The remaining terms are determined from the equations that were used to eliminate them during this solution process. Note that in this procedure one must be careful to get the correct quadrant for the phase of $(n\sigma\bar{t}_0)$.

These periodicity conditions are solved using the known solution of the linear vibration problem for free-flight, including both homogeneous and particular terms. For this system, the analytical results are sufficiently complicated that a purely analytical form is not presented. Instead, for each set of parameters selected, the conditions are enforced, the unknowns are obtained in the manner described above, and the non-penetration condition is checked (by direct simulation for one-half period, using the periodic initial conditions). In this manner, the steady-state impacting periodic response can be determined for any set of parameter values. For a typical set of response curves, one fixes all system parameters and varies σ over a range near the resonance of interest.

The stability of these symmetric periodic impacting responses can be determined in an analytical manner by examining the growth/decay of the small perturbations of the periodic responses [16, 17]. However, the calculations are cumbersome and not particularly enlightening, unless one is interested in the details of specific instabilities and bifurcations. Since the nonpenetrating condition (16) must be verified numerically in any case, we also examine stability numerically. In fact, it is found that the symmetric impacting response of interest is generally stable over much of the rotor speed near the resonance condition under consideration. However, it is observed that the system can undergo a grazing bifurcation [21] to chaos near resonance, leading to a situation that an analytical stability analysis is unable to handle. As shown in the following section, near this grazing bifurcation the absorber can undergo chatter-type responses, wherein several impacts occur over a short duration, and the absorber will come to rest relative to the primary structure, until the dynamic loads release it. However, these chaotic responses have very similar features, in terms of vibration amplitudes, to the periodic solution from which they arise, especially near resonance (the region of interest). This feature is a general result from the class of grazing bifurcation that occurs for this system [21, 25]. Therefore, we assume that the response curves generated by the periodic matching conditions provide an adequate approximation for evaluating the effects of absorber parameters on the system response throughout the resonance speed range—a conjecture confirmed by simulations.

We now turn to an analytical and simulation investigation of this system using a set of parameter values taken from an experimental study carried out by Duffy and co-workers at NASA [3].

5 Absorber Performance: Parameter Studies

5.1 System Parameters

For the results of this section we focus on parameter values derived from the experimental system considered by Duffy and co-workers [3]. Since the suppression of vibrations near resonance in the primary system is the main task of the absorber, we focus on the case where the rotor speed varies over a range that includes the resonant speed, and examine the effectiveness of the absorber for a range of applied torque levels. We also consider the effects of the absorber parameters, specifically, its mass, tuning, and coefficient of restitution, on the system response in order to offer guidelines for absorber designs. Response results will be compared for the system with the absorber locked versus the absorber free. In addition, simulations are employed to confirm the impacting analysis, and to examine regimes where the response is not so simple, for example, when the absorber chatters. We begin by describing how one distills the dimensionless parameters used in this study from the experimental data of Duffy [3]. Response curves and simulations are generated for these and nearby parameter values. From these results we draw some conclusions, which are presented in the following section.

The experimental studies described in [3] used a spin rig with a magnetic bearing to provide a sinusoidal excitation to the shaft. Two cantilevered plates were resonantly excited in this manner, and the absorbers consisted of spherical balls riding in circular troughs such that their motion was circular relative to the vibrating plate. The location and radius of the trough was selected to tune the absorber to a given engine order. Absorbers tuned to orders $n = 3, 4$, and 5 were tested; here we focus on the $n = 3$ case. Parameter values used in the present study are taken to be close to those taken from the $n = 3$ experiments. The plate has a length of approximately $L = 6.0$ inches, and the absorber mass is placed essentially at the end of the plate. The absorber is a sphere is of radius 0.0625 inches, and the trough radius is 1.031 inches, leading to an effective pendulum length of $d = 0.968$ inches. Thus, $\gamma = d/L = 0.16$. Taking the hub radius to be $R = 4.0$ inches (an estimate) yields $\delta = R/L = 0.67$. If we assume that the plate mass is an effective lumped mass at its free end, we have $L = \alpha L + d$, or $\alpha + \gamma = 1$ for this situation, so that $\alpha = 0.84$. By Eq. (13), this provides a tuning order of $\bar{n} = 3.07$, slightly higher than the $n = 3$ excitation. The absolute mass ratio used in [3] is 0.002 , but this does not account for the effective modal mass of the plate, which is taken to be concentrated at the end in our model. Using $1/3$ of the total plate mass for the effective modal mass yields $\mu = 0.006$. However, in the subsequent analysis and simulations it is observed that this value is too small to achieve good vibration reduction for the current model, so the typical value used in the present study is taken to be $\mu = 0.024$. For steel on steel impacts, a typical coefficient of restitution $e = 0.8$ is used. The plate natural frequency (at zero spin rate) was $\omega_0 = 282$ rad/sec, so that when the rotor speed gets near to $\Omega = 94$ rad/sec (900 rpm), third order excitation compo-

nents will cause a resonance in the plate. In terms of dimensionless parameters, the n^{th} order excitation frequency $n\sigma = n\Omega/\omega_0$ will match the (speed-dependent) natural frequency of the primary system when $n\sigma = \omega_{11}$. For the given parameter values, it is found that $\sigma_{res} \approx 0.345$.

5.2 System Response and Absorber Performance

For this study we perform simulation runs for various sets of parameter values guided by the NASA hardware. For these studies it is assumed that the excitation order, the absorber placement parameter, and the blade length to hub radius ratio are fixed, as follows: $n = 3$, $\alpha = 0.84$, $\delta = 0.67$. The design parameters are taken to be the absorber tuning \tilde{n} (or, equivalently, the nondimensional absorber effective length γ), the impact coefficient of restitution e , and the mass ratio μ . These will be varied near the nominal values of $\tilde{n} = 3$, $e = 0.8$, $\mu = 0.024$. For relevant ranges of these parameters the system response is determined over a range of rotor speeds σ for a range of excitation amplitudes f , focusing on the response near primary system resonance, $\sigma = 0.345$. In this manner we are able to determine general parameter trends that offer insight into absorber design guidelines.

We begin by showing in Fig. 8 a typical set of response curves, depicting various response features of the primary system and the absorber as the rotor speed is varied near resonance. In these plots results from both the analytically predicted stable and unstable symmetric impact motions are shown, along with reference plots (where appropriate) taken from the primary system with the absorber locked (the linear reference response). The quantity of primary interest is, of course, the vibration amplitude of the primary system, $|x|$, and it is seen that its resonance is reduced by the presence of the absorber. It should be noted that the impact response is measured by the values of x , \dot{x} , \dot{y} and t_0 at impact, and that these generally do not represent the peak amplitude. It is seen from the simulation results, however, that the impacts occur when the primary system is near its peak amplitude, so that this value is valid for comparing vibration amplitudes with and without the absorber.⁴

The details of the response near resonance are quite interesting, and, as noted above, may not be fully captured by the response curves predicted by the theory. Specifically, the existence of the symmetric impact motion depends on the non-penetration condition, Eq. (16), and this is, in fact, often violated near resonance. This arises from a grazing bifurcation, as now described. As the rotor speed is varied through resonance, the absorber dynamics undergo a sequence of transitions, as depicted in Fig. 9, which shows a series of steady-state absorber phase plane responses obtained by varying the rotor speed through resonance. Note that the symmetric impact motion develops a pair of interior loops which grow as the rotor speed is increased from just below

resonance. When these loops touch the $|y| = 1$ limits, a grazing bifurcation takes place that dramatically alters the qualitative nature of the response [21].⁵ Note that the response immediately after the grazing bifurcation is chaotic, and involves a number of small excursions near the barriers. In fact, some of these responses involve chatter, that is, the motion undergoes repetitive impacts of continually smaller velocity such that the absorber actually becomes stuck at the barrier in finite time and remains there for a duration. In this case the motion of the primary system holds the absorber in place until the constraint force goes to zero and changes sign, at which point the absorber is released from the barrier with zero relative velocity and continues its motion. The simulation of these events requires tracking this force, as described in the appendix.

As the rotor speed is decreased from above resonance, the same sequence of events is observed to occur. In fact, the upper and lower grazing bifurcations are very close to one another, and thus the chaos exists over a very narrow range of rotor speeds.

Some further details of a sample chaotic motion are shown in Fig. 10. This response has some interesting features, which are described here but not explored in detail. In particular, if one examines the chaos over a relatively short time interval, it appears to look like the chaotic example shown in Fig. 9. However, the long-term time behavior has a slow oscillation in the amplitude of the primary system response, as depicted in Fig. 10a, which shows $x(t)$ versus t over an interval corresponding to 3000 impacts, starting after 12,000 impacts have occurred. Figure 10b and Fig. 10c show projections of the Poincaré map (the one used to find the periodic impacting responses) for the same 3000 impacts. These show the four variables $(x, \dot{x}, \dot{y}, t_0)$ at the instants of impact at $y = 1$, where t_0 is the phase of the forcing, that is, $t_0 \bmod (2\pi/\omega)$. These Poincaré maps show that x indeed oscillates between lower and upper amplitudes, and remains bounded in an annular region. The absorber response is likewise bounded. The most interesting feature of this response is that there appear to be some invariant manifolds present, which trap the response for long periods of time, and along which the response traverses very slowly. These appear as the groups of points that collectively form the nearly-filled-out curves in the Poincaré map. While this response is interesting and deserving of further investigation, we do not pursue it here. It is sufficient for present purposes to note that the amplitude of the primary system response remains bounded by a value that is very near that of the underlying periodic response (which is penetrating, and thus non-physical, in this parameter range).

Since these chaotic responses have amplitudes that are very near those of the underlying periodic response, the absorber continues to function, even when the response is chaotic, and does

⁴This is a consequence of the phase relations dictated by the zero free flight damping.

⁵This grazing bifurcation is quite different in nature than the one wherein the symmetric impact motion merges with the linear non-impacting response. See [25] for a discussion of the classification of grazing bifurcations.

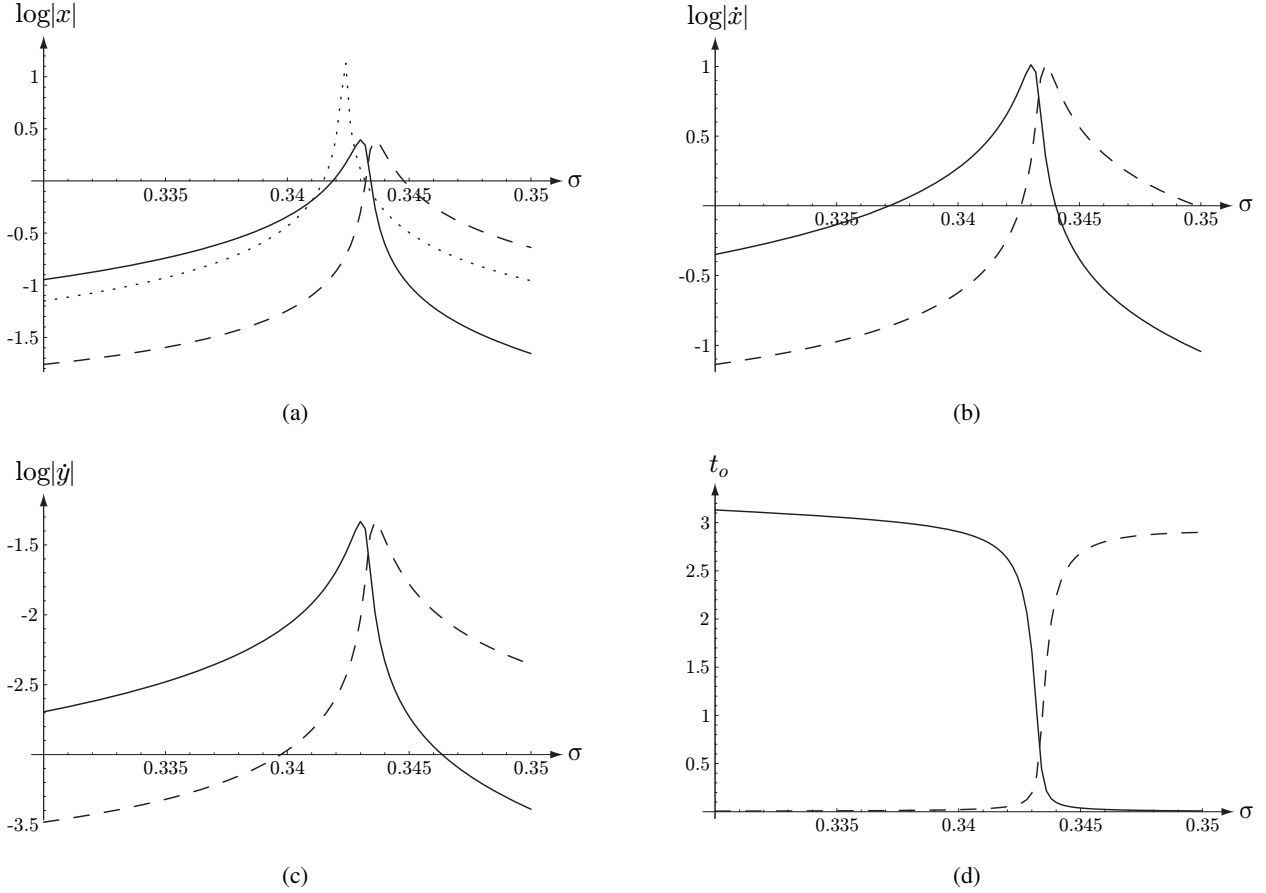


Figure 8. Symmetric impacting response versus rotor speed near primary system resonance, shown as the amplitudes of dynamic variables at impact. Solid lines represent the stable impacting response and dashed lines represent the unstable impacting response. Parameter values: $\delta = 0.67$, $\alpha = 0.84$, $e = 0.8$, $\mu = 0.024$, $\tilde{n} = 3.007$, $f = 0.005$, $n = 3$. (a) Primary system amplitude $\log_{10}|x|$, where the dotted line is the reference linear primary system response with the absorber locked, showing resonance. (b) Primary system velocity \dot{x} ; (c) Absorber velocity \dot{y} ; (d) Excitation phase t_0 .

so in a manner that is reasonably described by the (non-physical) periodic response predicted by the theory. In fact, these grazing bifurcations are observed to be of the type which immediately lead to chaotic responses that are closely related to their periodic source [25]. These chaotic oscillations generally grow in amplitude (relative to the underlying periodic response) as one moves beyond the bifurcation point. However, in the present system, another grazing bifurcation of exactly the same form takes place just above resonance, and thus the chaos exists only in a small range of rotor speeds near resonance. Since this is a very small window, it is valid to use the predicted periodic response to estimate the general amplitudes of vibration in the chaotic region, and thus over the entire region near resonance.

By using the predicted response curves for the impacting motions, one can carry out a systematic parameter study to determine the influence of the absorber parameters on the primary system response. This is carried out by the following procedure.

The parameters are set, the rotor speed is swept through resonance, and the peak amplitude of the primary system response is recorded. This is repeated over a range of force amplitudes, resulting in a curve that shows x_{\max} versus f . Figure 11a shows a set of such curves, generated for four values of the coefficient of restitution. Here it is seen that, as one might expect, more dissipation in the impacts leads to lower response amplitudes. Figure 11b shows a similar plot for four values of the absorber mass. Again, the expected result is obtained, showing that an increase in absorber mass lowers the primary system response amplitudes. Finally, in Fig. 11c, a similar plot is shown for three values of the absorber tuning which cover a wide range of tuning conditions. Here the results indicate that the peak primary system response appears to be quite insensitive to the absorber tuning. This may seem surprising, but it should be noted that the absorber is not really making use of its linear tuning while in its impact mode of operation.

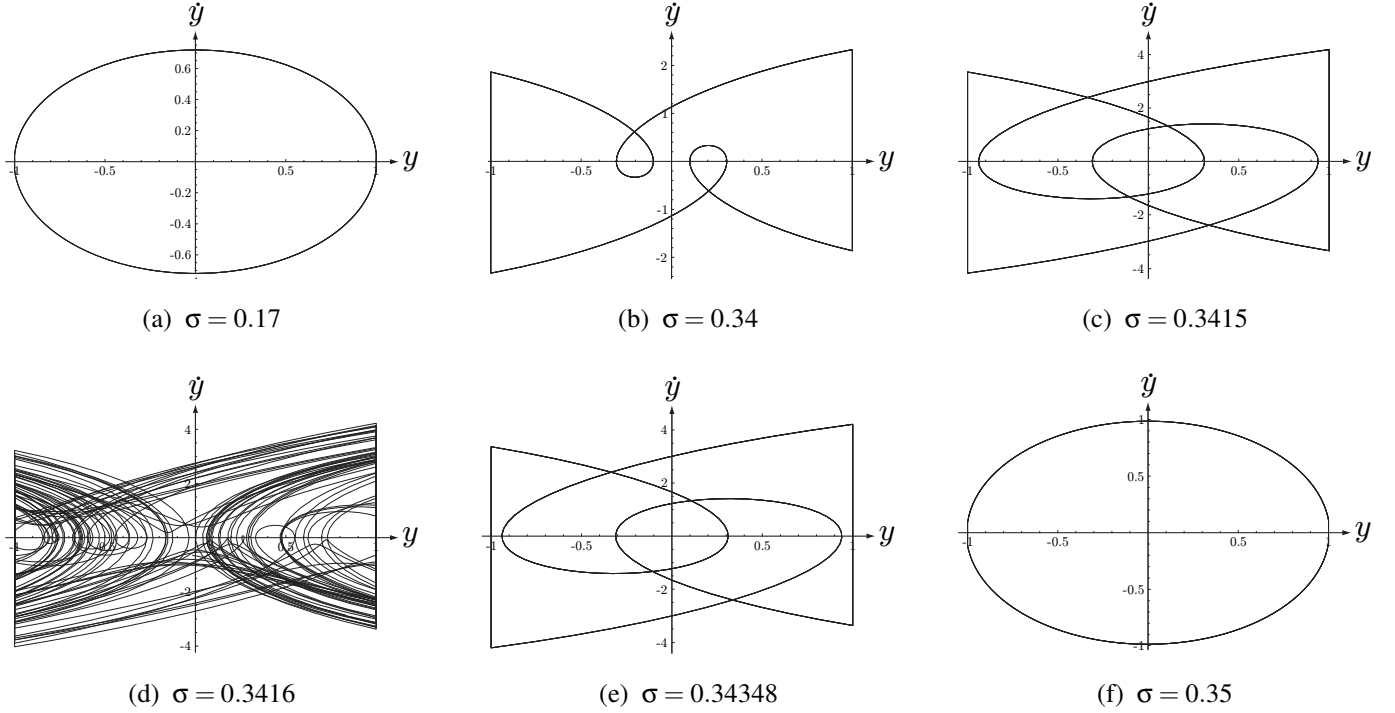


Figure 9. Representative absorber phase planes, \dot{y} versus y , showing steady-state responses. Parameter values: $\delta = 0.67$, $\alpha = 0.84$, $e = 0.8$, $\mu = 0.024$, $\tilde{n} = 3.007$, $f = 0.005$, $n = 3$. (a) Well below resonance, $\sigma = 0.17$; (b) just below resonance, $\sigma = 0.34$; (c) close to the first near-resonance grazing bifurcation, $\sigma = 0.3415$; (d) chaos, immediately beyond the grazing bifurcation, $\sigma = 0.3416$; (e) close to the second near-resonance grazing bifurcation, $\sigma = 0.34348$; (f) above resonance, near the grazing coincidence with the linear response, $\sigma = 0.35$.

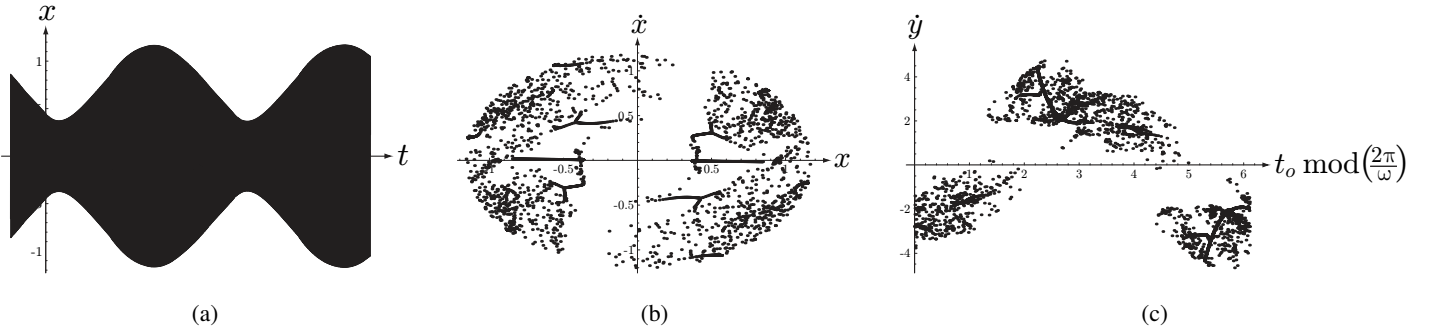


Figure 10. Some details of a typical chaotic response near resonance. Parameter values: $\delta = 0.67$, $\alpha = 0.84$, $e = 0.8$, $\mu = 0.024$, $\tilde{n} = 3.007$, $\sigma = 0.343$, $f = 0.005$, $n = 3$. (a) $x(t)$ versus t ; (b) $\dot{x}(t)$ versus $x(t)$ sampled at impact times; (c) $\dot{y}(t)$ versus the forcing phase, $t_o \bmod (2\pi/\omega)$, sampled at impact times.

Based on the latter observation, one may use a wide range of tunings and achieve similar performance if the absorber is to function in an impacting mode. In such cases, the design may be guided by other considerations, such as space constraints. However, if the absorber will function in its linear, non-impacting mode during some situations, then it should be tuned as closely as possible to the excitation order, but slightly below it, so that no resonance in the linear system is encountered as the rotor spins

up.

6 Conclusions and Directions for Future Work

In this study we have offered an investigation of tuned impact absorbers for reducing vibrations in rotating flexible structures. These absorbers have proven to be effective in experimental demonstrations, and the results presented here are a start to-

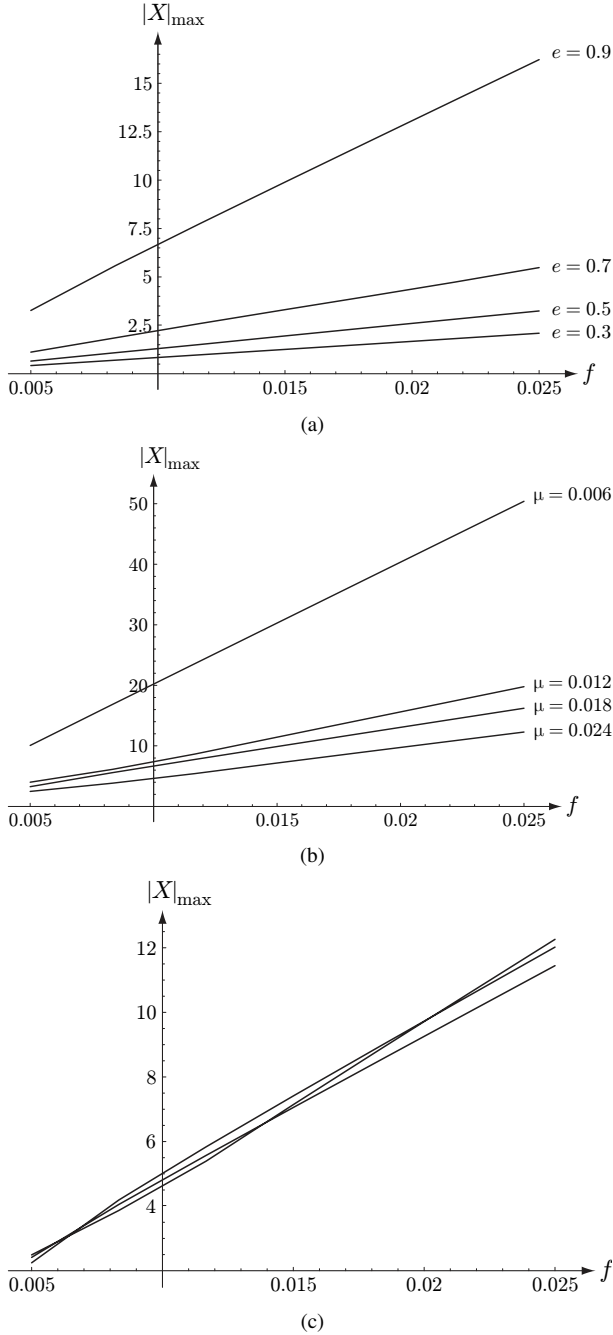


Figure 11. Peak response of the primary system near resonance versus force amplitude f , for $\delta = 0.67$, $\alpha = 0.84$, and $n = 3$: (a) $\mu = 0.024$, $\tilde{n} = 3.007$, and $e = 0.9, 0.7, 0.5, 0.3$; (b) $e = 0.8$, $\tilde{n} = 3.007$, and $\mu = 0.024, 0.018, 0.0120, 0.006$; (c) $\mu = 0.024$, $e = 0.8$, and $\tilde{n} = 2.81, 3.007, 3.28$.

wards the development of analytical tools for the prediction of their response characteristics and the manner in which these depend on system parameters.

The non-impacting linear response of the system is found to have some interesting features. Specifically, this two degree-of-freedom system will experience at most one resonance as the rotor speed is varied, and, in fact, if the absorber is slightly undertuned, one can avoid resonance altogether. The authors have studied in detail the response of linear system models of cyclicly coupled structures fitted with order-tuned absorbers in order to determine how these features are manifested in the coupled, multi-blade case [15]. Along these lines, it has been determined that the free flight damping of the primary system and the absorber may play an important role in the general features of the response, and this requires further study.

These absorbers, due to their small mass, are designed to operate in an impacting mode, and that is the main subject of this paper. It has been shown that the impact absorber is effective in reducing the response of the primary system near resonance, and that the performance of the absorber increases as one increases the mass ratio and reduces the coefficient of restitution. However, it was also found that the linear tuning of the absorber has little effect on performance, as might be expected, since one could use a simple rattling mass arrangement, with essentially zero restoring stiffness (that is, zero tuning) to achieve an impact damper. However, there is no detriment to using some linear tuning, so one might as well employ it to handle small levels of vibration.

Future work in this area should also include investigations that improve the model of the rotating flexible structure. These should incorporate single and multi-mode beam and plate models, possibly using finite elements, since impacts will typically excite higher modes. This may increase the predicted effectiveness of the impacts in damping resonant vibrations, since more energy can be transferred away from the resonant mode. In addition, the kinematics of the movement of the absorber relative to the flexible structure can be accounted for in such a model, which will allow one to account for nonlinear path effects. These effects can be designed so as to extend the non-impacting operating range of the absorber. Also, the well-know coupling between longitudinal and transverse motions in rotating beams can be taken into account [1]. The effects of damping in the primary structure and the absorber can also be included in an improved model, as can a more detailed consideration of the redistribution of blade stresses caused by the inclusion of the absorber [1]. These steps would lead to more accurate predictive tools for evaluating impact absorber designs for rotating structures. However, they would not be analytically tractable, and one would need to resort to simulation studies.

Further work could also include the use of multiple absorbers on a single flexible element. In addition, the response of systems of rotating coupled flexible structures, such as bladed disk assemblies and blisks (integrated blade/disk units) with ab-

sorbers is also of interest. As localization is known to occur in such systems when the subsystems are slightly mistuned from one another [26], it is of interest to know how sets of order-tuned and/or impact absorbers will perform in the face of these complex responses. An intriguing idea along these lines is to use sets of absorbers as a means of implementing intentional mistuning of the system, which has been suggested as a means of suppressing the damaging effects of localization [27]. And, of course, systematic experimentation is required before these devices can be proven to be of practical use.

ACKNOWLEDGMENT

This work was supported in part by grant CMS-0408866 from the National Science Foundation. SWS is grateful for visiting appointments at the University of Michigan, during which this work was initiated and largely carried out, and at the University of California-Santa Barbara, during which the work was completed. The authors would also like to thank Brian Olson for assistance with the preparation of the manuscript.

Appendix: The Constraint Force

It is of interest to investigate the situation when the absorber is held fixed relative to the primary system by dynamic effects, and the conditions for its release. This occurs in situations in which the absorber mass is held against one of the amplitude-limiting barriers by the motion of the primary system (typically after a completed chatter sequence). In these situations the oscillating motion of the primary system will eventually result in the release of the absorber, whereupon it continues its motion. In these cases one takes $y = \pm 1$ as the constraint. Another situation of interest is $y = 0$, which corresponds to the absorber locked in its central position. The response of the primary system for this reference case is considered in Section 3.1. In each of these cases a constraint force is required to hold the absorber in place. This force is of particular interest for the simulations, since it determines conditions for the occurrence of chatter and subsequent release of the absorber.

When the absorber is fixed at $y = \hat{y}$ ($\hat{y} = +1, -1, \text{ or } 0$), the equations of motion are given by Eq. (1) with $y = \hat{y}$, $\dot{y} = 0$, and an applied force of

$$\mathbf{F} = (f \cos(n\sigma\tau), F_c), \quad (17)$$

where F_c is the constraint force. One can eliminate $\ddot{x}(\tau)$ from these equations, resulting in an expression for F_c in terms of \hat{y} , $x(\tau)$, $f \cos(n\sigma\tau)$, and the system parameters. Chatter can lead to difficulties in the simulations, since a large number of impacts occur over an arbitrarily small time duration, after which the resulting system has a smaller number of degrees of freedom. In

these cases, when the absorber impacts become sufficiently close together (as determined by a user-defined small parameter), one can set y to the corresponding limit (± 1), use the constrained equation of motion for $x(\tau)$, and track F_c as a function of τ . At the time when F_c goes to zero, the absorber is released from the barrier with $\dot{y} = 0$, whereupon simulation of the full two degree of freedom system can resume, using the system states at release for the “reset” initial conditions.

REFERENCES

- [1] Wang, Y., Chao, C. P., and Shaw, S. W., 1997. “Design of pendulum vibration absorbers for the attenuation of transverse vibrations in rotating beams”. In Proceedings of the ASME 17th Biennial Conference on Mechanical Vibration and Noise, no. DETC97/VIB-4182.
- [2] Hollkamp, J. J., Bagley, R. L., and Gordon, R. W., 1999. “A centrifugal pendulum absorber for rotating, hollow engine blades”. *Journal of Sound and Vibration*, **219**(3), pp. 539–549.
- [3] Duffy, K. P., Bagley, R. L., and Mehmed, O., 2000. “On a self-tuning impact vibration damper for rotating turbomachinery”. In 36th AIAA/ASME/SAE/ASEE Joint Propulsion Conference and Exhibit, no. AIAA-2000-3100.
- [4] Ker Wilson, W., 1968. *Practical Solutions of Torsional Vibration Problems*, 3rd ed., Vol. IV. Chapman and Hall Ltd, London, ch. XXX.
- [5] Nester, T. M., Haddow, A. G., Shaw, S. W., Brevick, J. E., and Borowski, V. J., 2003. “Vibration reduction in variable displacement engines using pendulum absorbers”. In Proceedings of the SAE Noise and Vibration Conference and Exhibition, no. 2003-01-1484. Paper 2003-01-1484.
- [6] Newland, D. E., 1964. “Nonlinear aspects of the performance of centrifugal pendulum vibration absorbers”. *Journal of Engineering for Industry*, **86**, pp. 257–263.
- [7] Alsuwaiyan, A. S., and Shaw, S. W., 2002. “Performance and dynamic stability of general-path centrifugal pendulum vibration absorbers”. *Journal of Sound and Vibration*, **252**(5), pp. 791–815.
- [8] Denman, H. H., 1992. “Tautochronic bifilar pendulum torsion absorbers for reciprocating engines”. *Journal of Sound and Vibration*, **159**(2), pp. 251–277.
- [9] Chao, C. P., Lee, C. T., and Shaw, S. W., 1997. “Stability of the unison response for a rotating system with multiple centrifugal pendulum vibration absorbers”. *Journal of Applied Mechanics*, **64**, pp. 149–156.
- [10] Chao, C. P., Lee, C. T., and Shaw, S. W., 1997. “Non-unison dynamics of multiple centrifugal pendulum vibration absorbers”. *Journal of Sound and Vibration*, **204**(5), pp. 769–794.
- [11] Madden, J. F. Constant frequency bifilar vibration absorber. United States Patent No. 4218187.

- [12] Alsuwaiyan, A., and Shaw, S. W., 2003. “Steady-state response of systems of nearly-identical torsional vibration absorbers”. *Journal of Vibration and Acoustics*, **125**(1), pp. 80–87.
- [13] Ewins, D. J., 1973. “Vibration characteristics of bladed disc assemblies”. *Journal of Mechanical Engineering Science*, **15**(3), pp. 165–186.
- [14] Pierre, C., 1988. “Mode localization and eigenvalue loci veering phenomena in disordered structures”. *Journal of Sound and Vibration*, **126**(3), pp. 485–502.
- [15] Olson, B., Shaw, S., and Pierre, C., 2005. “Order-tuned vibration absorbers for cyclic rotating flexible structures”. In Proceedings of the 2005 ASME Design Engineering Technical Conferences, 20th Biennial Conference on Mechanical Vibration and Noise, no. DETC2005-84641.
- [16] Masri, S., and Caughey, T. K., 1966. “On the stability of the impact damper”. *Journal of Applied Mechanics*, **33**, pp. 586–592.
- [17] Shaw, J., and Shaw, S. W., 1989. “The onset of chaos in a two-degree-of-freedom impacting system”. *Journal of Applied Mechanics*, **56**, pp. 168–174.
- [18] Den Hartog, J. P., 1938. “Tuned pendulums as torsional vibration eliminators”. In *Stephen Timoshenko 60th Anniversary Volume*. The Macmillan Company, New York, pp. 17–26.
- [19] Sharif-Bakhtiar, M., and Shaw, S. W., 1988. “The dynamic response of a centrifugal pendulum vibration absorber with motion-limiting stops”. *Journal of Sound and Vibration*, **126**(2), pp. 221–235.
- [20] Shaw, S. W., and Holmes, P. J., 1983. “A periodically forced piecewise linear oscillator”. *Journal of Sound and Vibration*, **90**(1), pp. 129–155.
- [21] Nordmark, A., 2001. “Existence of periodic orbits in grazing bifurcations of impacting mechanical oscillators”. *Nonlinearity*, **14**, pp. 1517–1542.
- [22] Whiston, G. S., 1992. “Singularities in vibro-impact dynamics”. *Journal of Sound and Vibration*, **152**(3), pp. 427–460.
- [23] Peterka, F., 1999. “Analysis of motion of the impact-dry-friction pair of bodies and its application to the investigation of the impact dampers dynamics”. In Proceedings of the 1999 ASME Design Engineering Technical Conferences, no. DETC99/VIB-8350.
- [24] Senator, M., 1970. “Existence and stability of periodic motions of a harmonically forced impacting system”. *Journal of the Acoustical Society of America*, **47**, pp. 1390–1397.
- [25] Chin, W., Ott, E., Nusse, H., and Grebogi, C., 1995. “Universal behavior of impact oscillators near grazing incidence”. *Physics Letters A*, **201**, pp. 197–204.
- [26] Wei, S. T., and Pierre, C., 1988. “Localization phenomena in mistuned assemblies with cyclic symmetry part ii: Forced vibrations”. *Journal of Vibration, Acoustics, Stress, and Reliability in Design*, **110**, pp. 439–449.
- [27] Castanier, M. P., and Pierre, C., 2002. “Using intentional mistuning in the design of turbomachinery rotors”. *AIAA Journal*, **40**(10), pp. 2077–2086.